Monthly Notices
of the
ROYAL ASTRONOMICAL SOCIETY

MNRAS **492,** 3032–3040 (2020)
Advance Access publication 2020 January 16

doi:10.1093/mnras/staa066

Searching for optical companions to four binary millisecond pulsars with the Gran Telescopio Canarias

A. Yu. Kirichenko [1,2★] A. V. Karpova [2★] D. A. Zyuzin [2] S. V. Zharikov [1] E. A. López [3] Yu. A. Shibanov,[2] P. C. C. Freire [4] E. Fonseca[5] and A. Cabrera-Lavers[6,7]

[1]*Instituto de Astronomía, Universidad Nacional Autónoma de México, Apdo. Postal 877, 22800 Baja California, Mexico*
[2]*Ioffe Institute, Politekhnicheskaya 26, St Petersburg 194021, Russia*
[3]*Instituto de Investigación en Ciencias Físicas y Matemáticas, USAC, Ciudad Universitaria, 01012, Zona 12, Guatemala*
[4]*Max-Planck-Institut für Radioastronomie, Auf dem Hügel 69, D-53131 Bonn, Germany*
[5]*Department of Physics and McGill Space Institute, McGill University, 3600 University Street, Montreal, QC H3A 2T8, Canada*
[6]*Instituto de Astrofísica de Canarias, Vía Láctea s/n, E-38200 La Laguna, Tenerife, Spain*
[7]*GRANTECAN, Cuesta de San José s/n, E-38712 Breña Baja, La Palma, Spain*

Accepted 2020 January 8. Received 2020 January 7; in original form 2019 November 11

ABSTRACT

We report on multiband photometric observations of four binary millisecond pulsars with the Gran Telescopio Canarias. The observations led to detection of binary companions to PSRs J1630+3734, J1741+1351, and J2042+0246 in the Sloan g', r', and i' bands. Their magnitudes in the r' band are ≈24.4, 24.4, and 24.0, respectively. We also set a 3σ upper limit on the brightness of the PSR J0557+1550 companion in the r' band of ≈25.6 mag. Combining the optical data with the radio timing measurements and white dwarf cooling models, we show that the detected companions are cool low-mass white dwarfs with temperatures and ages in the respective ranges of (4–7) × 10^3 K and 2–5 Gyr. All the detected white dwarfs are found to likely have either pure hydrogen or mixed helium–hydrogen atmospheres.

Key words: binaries: general – pulsars: individual: PSR J0557+1550 – pulsars: individual: PSR J1630+3734 – pulsars: individual: PSR J1741+1351 – pulsars: individual: PSR J2042+0246.

1 INTRODUCTION

Millisecond pulsars (MSPs) represent a subclass of radio pulsars that are characterized by short rotational periods ($P < 30$ ms) and low spin-down rates ($\dot{P} \sim 10^{-19}$–10^{-20} s s^{-1}). To date, about 400 MSPs have been detected.[1] According to the commonly accepted 'recycling' scenario, such objects are formed as 'normal' pulsars in binary systems and then are spun-up due to accretion of matter from companion stars (Bisnovatyi-Kogan & Komberg 1974; Alpar et al. 1982). Resulting systems have essentially circular orbits and 'peeled' companions, usually low-mass white dwarfs (WDs; e.g. Tauris 2011). To explain binary MSPs with eccentric orbits, other formation channels are discussed such as the triple-system formation scenario and the direct formation via a delayed accretion-induced collapse of massive WDs (Portegies Zwart et al. 2011; Tauris 2011; Freire & Tauris 2014). Some other possibilities for the origin of these systems are discussed by Antoniadis (2014).

Under certain conditions, which are usually defined by the timing noise and MSP binary period, the fundamental parameters of MSP systems, including masses and system inclinations, can be derived from radio timing measurements of the relativistic Shapiro delay (Shapiro 1964). Otherwise, combination of timing and optical studies is needed. In case of a WD or a 'spider' class companion, optical observations are crucial for understanding its nature and evolution of the binary system (van Kerkwijk et al. 2005). Comparison of optical data with WD theoretical cooling models can provide its parameters, such as chemical composition of WD atmosphere, mass, temperature, age, and radial velocity (in case of phase-resolved spectroscopic observations). Combined together with the timing results, this allows one to set constraints on the mass of a neutron star (van Kerkwijk et al. 2005; Antoniadis et al. 2012, 2013). On the other hand, if masses of a binary system components are determined with a high precision from the radio timing, optical observations are useful to constrain other parameters. For instance, complemented by the radio timing constraints and the theoretical predictions, optical photometric and spectroscopic observations allow one to constrain the distance independently of the radio parallax and dispersion measure (DM) models. For all these reasons, recent gamma-ray and radio discoveries of MSP binaries have

★ E-mail: aida.taylor@gmail.com (AYK); annakarpova1989@gmail.com (AVK)
[1]https://apatruno.wordpress.com/about/millisecond-pulsar-catalogue/

Table 1. Parameters of the binary MSP systems studied in this paper. Numbers in parentheses are 1σ uncertainties related to the last significant digits quoted. $D_{\rm YMW16}$ is the DM distance derived using the YMW16 (Yao, Manchester & Wang 2017) Galactic electron density model.[a] $D_{\rm p}$ is the timing parallax distance.

MSP	J0557+1550	J1630+3734	J1741+1351	J2042+0246
Right ascension α (J2000)	$05^{\rm h}57^{\rm m}31\overset{\rm s}{.}44918(9)$	$16^{\rm h}30^{\rm m}36\overset{\rm s}{.}46693(7)$	$17^{\rm h}41^{\rm m}31\overset{\rm s}{.}144731(2)$	$20^{\rm h}42^{\rm m}11\overset{\rm s}{.}00287(5)$
Declination δ (J2000)	$15^\circ50'06\overset{''}{.}046(8)$	$37^\circ34'42\overset{''}{.}097(1)$	$13^\circ51'44\overset{''}{.}12188(4)$	$02^\circ46'14\overset{''}{.}397(2)$
Galactic longitude l ($^\circ$)	192.68	60.24	37.89	48.99
Galactic latitude b ($^\circ$)	−4.31	43.21	21.64	−23.02
Proper motion $\mu_\alpha = \dot{\alpha}\cos\delta$ (mas yr^{-1})	–	2.4(3.5)	−8.98(2)	15.1(1.2)
Proper motion μ_δ (mas yr^{-1})	–	−15.9(3.4)	−7.42(2)	−14.1(3.5)
Epoch (MJD)	56346	56136	56209	56520
Spin period P (ms)	2.5563670767830(5)	3.3181121293936(9)	3.7471545002599400 30(7)	4.5337267023282(3)
Period derivative $\dot{P}$ (10^{-20} s s^{-1})	0.735(2)	1.077(9)	3.021648(14)	1.403(6)
Characteristic age $\tau = P/2\dot{P}$ (Gyr)	5.5	4.9	2.0	5.1
Orbital period $P_{\rm b}$ (d)	4.846550440(4)	12.52502574(2)	16.335347828(4)	77.2005806(3)
Projected semimajor axis x (lt-s)	4.0544597(8)	9.039336(1)	11.0033159(5)	24.5699969(8)
Spin-down power $\dot{E}$ (erg s^{-1})	1.7×10^{34}	1.2×10^{34}	2.3×10^{34}	5.9×10^{33}
Dispersion measure (DM; pc cm^{-3})	102.6	14.2	24.2	9.3
Distance $D_{\rm YMW16}$ (kpc)	1.83	1.19	1.36	0.64
Timing parallax (mas)	–	–	0.6(1)	–
Distance $D_{\rm p}$ (kpc)	–	–	$1.8^{+0.5}_{-0.3}$	–
Companion mass $M_{\rm c}$ ($M_\odot$)	$\geq 0.2^b$	$\geq 0.24^b$	$0.22^{+0.05}_{-0.04}$	$\geq 0.19^b$
Pulsar mass $M_{\rm p}$ ($M_\odot$)	–	–	$1.14^{+0.43}_{-0.25}$	–
System inclination i ($^\circ$)	–	–	73^{+3}_{-4}	–
References[c]	[1]	[2]	[3]	[2]

[a]In the case of the NE2001 model (Cordes & Lazio 2002), the distances $D_{\rm NE2001}$ are 2.92 (J0557+1550), 0.94 (J1630+3734), 0.9 (J1741+1351), and 0.83 (J2042+0246) kpc.
[b]A minimum companion mass is calculated assuming the inclination angle of the binary orbit $i = 90^\circ$ and the pulsar mass $M_{\rm p} = 1.4\,M_\odot$.
[c]Parameters are obtained from [1] – Scholz et al. (2015), [2] – Sanpa-Arsa (2016), and [3] – Arzoumanian et al. (2018) (see also https://data.nanograv.org for current values).

triggered intensive studies with large optical telescopes (Bassa et al. 2016; Dai et al. 2017; Kirichenko et al. 2018; Beronya et al. 2019).

In this paper, we present the results of first deep optical observations of four binary MSPs with the Gran Telescopio Canarias (GTC): PSRs J0557+1550, J1630+3734, J1741+1351, and J2042+0246. The parameters of the systems and their previous studies are reviewed in Section 2. In Section 3, we provide a description of our optical observations and data reduction, and the results are presented in Section 4 and are discussed in Sections 4 and 5.

2 TARGETS

The parameters of the four MSP systems are collected in Table 1. For each of them, the orbital period $\gtrsim$4 d together with the companion mass or its lower limit of $\geq$0.19 $M_\odot$ derived from the radio timing imply that the companion is likely a WD. We have selected these systems for optical observations considering the WD nature of the companions and distances $\lesssim$2 kpc. Below we shortly describe previous studies of the targets.

PSR J0557+1550 was discovered in the PALFA Galactic plane survey using the Arecibo Radio Telescope (Scholz et al. 2015). The authors did not find any optical or infrared counterpart to the pulsar in the SIMBAD data base and concluded that the apparent visual magnitude of its companion has to be >22.

PSRs J1630+3734 and *J2042+0246* were discovered in the radio observations of *Fermi* unassociated sources (Ray et al. 2012; Sanpa-Arsa 2016). The most recent timing analyses of these pulsars were performed by Sanpa-Arsa (2016). After inspecting archival data from the Catalina Sky Survey with limiting visual magnitudes of 19.5–21.5, Salvetti et al. (2017) have reported non-detection of the PSR J1630+3734 companion.

PSR J1741+1351 was discovered with the Parkes Radio Telescope (Jacoby et al. 2007) and the first Shapiro delay measurements for this pulsar were performed by Freire et al. (2006). It was also detected in gamma-rays with the *Fermi* telescope (Espinoza et al. 2013). Using the 11-yr data set from the North American Nanohertz Observatory for Gravitational Waves (NANOGrav), Arzoumanian et al. (2018) measured masses of both PSR J1741+1351 and its companion and the system inclination (see Table 1). Our optical detection of the companion with the GTC and its preliminary analysis have been briefly reported in a conference paper (Zyuzin et al. 2019).

3 OBSERVATIONS AND DATA REDUCTION

The fields of PSRs J0557+1550, J1630+3734, J1741+1351, and J2042+0246 were observed[2] in 2018 June, September, and October under clear sky conditions using the Optical System for Imaging and low Resolution Integrated Spectroscopy (OSIRIS)[3] instrument at the GTC. OSIRIS consists of two CCDs and provides a field of view (FoV) of 7.8 × 7.8 arcmin^2 and a pixel scale of 0.254 arcsec. To avoid affection by bad pixels, 5 arcsec dithering between the individual exposures was used in all observing programmes. In addition, short 20 s exposures of each pulsar field in the r' band were obtained to avoid saturation of bright stars that were further used for precise astrometry. The details of the observations are presented in Table 2.

We performed standard data reduction, including bias subtraction and flat-fielding, using the Image Reduction and Analysis Facility

[2]Programmes GTC4-18AMEX and GTC20-18BMEX, PI: A. Kirichenko.
[3]http://www.gtc.iac.es/instruments/osiris/

Table 2. Log of the Gran Telescopio Canarias (GTC) observations.

Filter	Exposure time (s)	Airmass	Seeing (arcsec)	Zero-point	Date (dd-mm-yyyy)	MJD
			PSR J0557+1550			
r'	120 × 12	1.06–1.10	0.7–0.8	29.02(1)	14-10-2018	58405
			PSR J1630+3734			
g'	200 × 15	1.02–1.06	0.7–0.8	28.77(2)	06-06-2018	58275
r'	120 × 22	1.03–1.09	0.7–0.8	28.96(1)	05-06-2018	58274
i'	120 × 23	1.09–1.21	0.7–0.8	28.59(1)	05-06-2018	58274
			PSR J1741+1351			
g'	200 × 15	1.04–1.08	0.7–1.1	28.66(2)	06-06-2018	58275
r'	120 × 29	1.13–1.34	0.8–1.3	28.99(1)	13-06-2018	58282
i'	120 × 23	1.13–1.29	0.7–0.9	28.55(1)	05-06-2018	58274
			PSR J2042+0246			
g'	200 × 15	1.11–1.12	0.7–0.8	28.75(2)	03-09-2018	58364
r'	120 × 23	1.12–1.18	0.6–0.7	28.98(1)	03-09-2018	58364
i'	120 × 23	1.12–1.20	0.6–0.9	28.55(1)	03-09-2018	58364

(IRAF) package. The cosmic rays were removed from each individual exposure with the L.A.COSMIC algorithm (van Dokkum 2001). For each field and filter, the individual images were then aligned to the best quality image and combined. The four targets were exposed on CCD2 providing a FoV of 3.9 × 7.8 arcmin^2. All necessary astrometry and photometry calibrations were performed focusing on this part of the detector.

The astrometric solutions for the four pulsar fields were computed using the short exposures. Sets of 16–30 relatively bright stars from the *Gaia* Data Release 2 (DR2) catalogue (Gaia Collaboration et al. 2016, 2018) detected with the signal-to-noise ratios $\gtrsim$20 were used as the Web Coverage Service (WCS) references. Their position uncertainties on the images and catalogue uncertainties were $\lesssim$50 and $\lesssim$1 mas, respectively. OSIRIS contains geometrical distortions increasing with the distance from the detector aimpoint where the targets were exposed. This hampers the accurate astrometric transformation. To minimize distortion effects, the reference stars for PSRs J0557+1550, J1741+1351, and J2042+0246 fields were selected within 1 arcmin of the target positions, numbering 23, 19, and 16, respectively. For PSR J1630+3734, which has the largest Galactic latitude, there are no sufficient suitable reference objects in its immediate vicinity, and we used 30 stars within 4 arcmin of its position. In addition, to obtain the astrometric fits, we have followed the 'general' scheme (linear terms plus distortion) described in the OSIRIS User Manual.[4] We used the CCMAP routine, which includes the frame shift, rotation, and scale factor defined as recommended in the manual. Formal rms uncertainties of the resulting astrometric fits are presented in Table 3. They are compatible with the position uncertainties of reference stars on the images. Selection of a larger amount of reference stars and choosing their different sets did not change the solutions significantly. The resulting solutions were applied to the combined images.

The photometric referencing was obtained using Sloan standards SA 104-428, SA 110-232, and SA 112-805 from Smith et al. (2002) observed during the same nights as our targets in all respective bands. To determine the magnitude zero-points, we used their measured magnitudes and the mean OSIRIS atmosphere extinction coefficients $k_{g'} = 0.15 \pm 0.02$, $k_{r'} = 0.07 \pm 0.01$, and $k_{i'} = 0.04 \pm 0.01$. To verify the obtained calibration, we have compared the magnitudes of several stars in the pulsar fields against those in the Sloan Digital Sky Survey (SDSS) and Panoramic Survey Telescope and Rapid Response System (Pan-STARRS) Data Release 1 (DR1) catalogues for all bands. In most of the cases, the OSIRIS and the catalogue magnitudes were consistent within uncertainties. The only discrepancy of ≈0.1 mag was found for the g'-band magnitudes of the PSR J1741+1351 field stars, implying a slightly variable transparency during the night of observations, and we have taken it into account in our calculations. The resulting zero-points are presented in Table 2.

[4]http://www.gtc.iac.es/instruments/osiris/media/OSIRIS-USER-MANUAL_v3_1.pdf

4 RESULTS AND DISCUSSION

The resulting ∼23 × 23 arcsec^2 r'-band images of the four pulsar fields are presented in Fig. 1. The crosses correspond to the pulsar positions obtained from the radio timing and shifted according to proper motions to match the epoch of the optical observations, where respective information on the proper motion is provided. The astrometric uncertainties are negligible in the spatial scale of the optical images.

In the fields of PSRs J1630+3734, J1741+1351, and J2042+0246 in all bands we firmly detect star-like objects, whose coordinates coincide with the pulsar positions (see also Table 3). To calculate the probability of an accidental coincidence of pulsar positional regions with unrelated field objects, we have used the Poisson distribution $P = 1 - \exp(-\pi\sigma R^2)$, where σ and R correspond to the surface number density of stars with a similar magnitude and the astrometric accuracy, respectively. Considering magnitudes in a range of 19–25, in all cases this probability does not exceed ≈10^{-2}. For this reason, below we consider the detected objects as optical binary companions of the MSPs. Two of them, companions to PSRs J1741+1351 and J2042+0246, show star-like profiles, while the PSR J1630+3734 companion profile is more complex. The point spread function (PSF) subtraction of this source using the IRAF/DAOPHOT ALLSTAR routine has revealed a faint slightly extended underlying object located about 1 arcsec north-east from the source maximum peak. It is enlarged in the left-hand bottom corner of the right-hand upper panel of Fig. 1, where the companion was subtracted. The PSF photometry and iterative PSF

Table 3. Astrometric and photometric information for the MSP systems and the interstellar reddening in their direction. Reddening, intrinsic colours, and absolute magnitudes are provided for the latest published distance estimations, i.e. DM distances for PSRs J0557+1550, J1630+3734, and J2042+0246 based on the YMW16 model and the timing parallax distance for PSR J1741+1351 (see Table 1). α_p and δ_p are the pulsars' coordinates for the epoch of the GTC observations (errors include uncertainties of the radio positions and proper motion that are negligible in comparison with the rms uncertainties of the GTC astrometric fits). α_c, $\Delta\alpha_c$ and δ_c, $\Delta\delta_c$ are coordinates of the optical companions on the images and their rms uncertainties.

MSP	J0557+1550	J1630+3734	J1741+1351	J2042+0246
α_p (J2000)	$05^h57^m31\overset{s}{.}44918(9)$	$16^h30^m36\overset{s}{.}468(2)$	$17^h41^m31\overset{s}{.}141245(8)$	$20^h42^m11\overset{s}{.}0080(4)$
δ_p (J2000)	$15°50'06\overset{''}{.}046(8)$	$37°34'42\overset{''}{.}00(2)$	$13°51'44\overset{''}{.}0799(1)$	$02°46'14\overset{''}{.}33(2)$
α_c (J2000)	–	$16^h30^m36\overset{s}{.}475$	$17^h41^m31\overset{s}{.}144$	$20^h42^m11\overset{s}{.}005$
δ_c (J2000)	–	$37°34'41\overset{''}{.}92$	$13°51'43\overset{''}{.}95$	$02°46'14\overset{''}{.}46$
rms $\Delta\alpha_c$ (arcsec)	0.05	0.02	0.05	0.04
rms $\Delta\delta_c$ (arcsec)	0.04	0.02	0.05	0.05
g'	–	25.43(4)	24.74(5)	24.96(4)
r'	>25.6	24.44(4)	24.38(4)	23.97(2)
i'	–	24.17(4)	24.17(4)	23.58(3)
$E(B-V)^a$	$0.19^{+0.03}_{-0.01}$	$0.00^{+0.01}_{-0.00}$	$0.12^{+0.01}_{-0.03}$	0.07 ± 0.02
$A_{g'}$	–	$0.00^{+0.03}_{-0.00}$	$0.42^{+0.03}_{-0.10}$	0.26 ± 0.07
$A_{r'}$	$0.48^{+0.07}_{-0.02}$	$0.00^{+0.02}_{-0.00}$	$0.30^{+0.02}_{-0.07}$	0.18 ± 0.05
$A_{i'}$	–	$0.00^{+0.02}_{-0.00}$	$0.22^{+0.02}_{-0.05}$	0.14 ± 0.03
$(g'-r')_0$	–	$0.99^{+0.07}_{-0.06}$	$0.24^{+0.07}_{-0.14}$	0.93 ± 0.10
$(r'-i')_0$	–	$0.27^{+0.06}_{-0.06}$	$0.13^{+0.06}_{-0.10}$	0.35 ± 0.07
$M_{r'}$	>13.8	14.06 ± 0.04	$12.80^{+0.44}_{-0.61}$	14.76 ± 0.05
Effective temperature $T_{\rm eff}$ (K)	$\lesssim 5.0 \times 10^3$	$\sim 4 \times 10^3$	$\sim (6–7) \times 10^3$	$4.49(14) \times 10^3$
Cooling age t (Gyr)	$\gtrsim 1.5$	~2–5	~1–2	$5.6^{+0.9}_{-1.2}$

[a]In the directions to PSRs J1630+3734 and J2042+0246 the reddening is the same for the DM distance estimations provided either by the YMW16 or NE2001 models. For PSR J1741+1351, $E(B-V)$ does not vary for $D > 0.9$ kpc.

subtraction were applied both to the companion and this source to measure their magnitudes and positions. The underlying object is detected at about 3σ significance in the r' and i' bands with a magnitude of ≈26.5 and is not detected in the g' band down to the ≈27.5 mag limit. Its relation to the pulsar companion remains unclear. It is likely that the object is a hint of a distant galaxy. The resulting observed magnitudes of the proposed companions are presented in Table 3.

As the PSR J0557+1550 companion is undetected in the only available r' band, we have estimated a 3σ upper limit on its brightness in this band (see Table 3).

To calculate the absolute magnitudes and intrinsic colours of the optical companions, we used the 3D map of interstellar dust reddening $E(B-V)$ that is based on the Pan-STARRS 1 and Two Micron All-Sky Survey (2MASS) stellar photometry and *Gaia* parallaxes (Green et al. 2019).[5] Using distances to the pulsars from Table 1, we obtained the corresponding $E(B-V)$ colour excesses (Table 3). They were then converted to the extinction corrections $A_{g',r',i'}$ for all the bands utilizing coefficients provided by Schlafly & Finkbeiner (2011). The resulting corrections, absolute magnitudes, and intrinsic colours are presented in Table 3.

As we noted in Section 2, the companions to the pulsars are likely WDs. To verify this, we compared the obtained absolute magnitudes and dereddened colours with the cooling models of helium-core WDs with hydrogen atmospheres (Althaus, Miller Bertolami & Córsico 2013)[6] and CO-core WDs with hydrogen and helium atmospheres (known as the Bergeron models; Holberg & Bergeron 2006; Kowalski & Saumon 2006; Bergeron et al. 2011; Tremblay, Bergeron & Gianninas 2011).[7] The corresponding colour–magnitude and colour–colour diagrams are presented in Fig. 2, where evolutionary sequences for WDs of different classes are shown by different line types. The positions of the detected companions in the diagrams, particularly in the colour–magnitude diagram, depend on the accepted distances to the pulsars. To account for different possibilities, for each pulsar we show at least two positions, corresponding to the DM distances based on the NE2001 and YMW16 Galactic electron density distribution models (see Table 1). For PSR J1741+1351, we also include the point corresponding to the parallactic distance from Arzoumanian et al. (2018). Bellow we analyse the results obtained for each object.

4.1 PSR J0557+1550

PSR J0557+1550 was observed only in the r' band and no optical source was detected at its radio position down to $r' \geq 25.6$ mag. Comparison of the lower limit on $M_{r'}$ (see Table 3, $D_{\rm YMW16} = 1.83$ kpc) with the cooling models for a hydrogen-atmosphere WD with the minimum companion mass ≈0.2 $M_\odot$ implies the age $t \gtrsim 1.5$–3 Gyr and the WD effective temperature $T_{\rm eff} \lesssim (4.6–5.0) \times 10^3$ K. The respective values for the distance $D_{\rm NE2001} = 2.92$ kpc, which is based on the NE2001 model, are $M_{r'} > 12.6$, $t \gtrsim 1$–2 Gyr, and $T_{\rm eff} \lesssim (5.7–6.3) \times 10^3$ K.

[5]http://argonaut.skymaps.info/

[6]http://evolgroup.fcaglp.unlp.edu.ar/TRACKS/tracks_heliumcore.html

[7]http://www.astro.umontreal.ca/ bergeron/CoolingModels

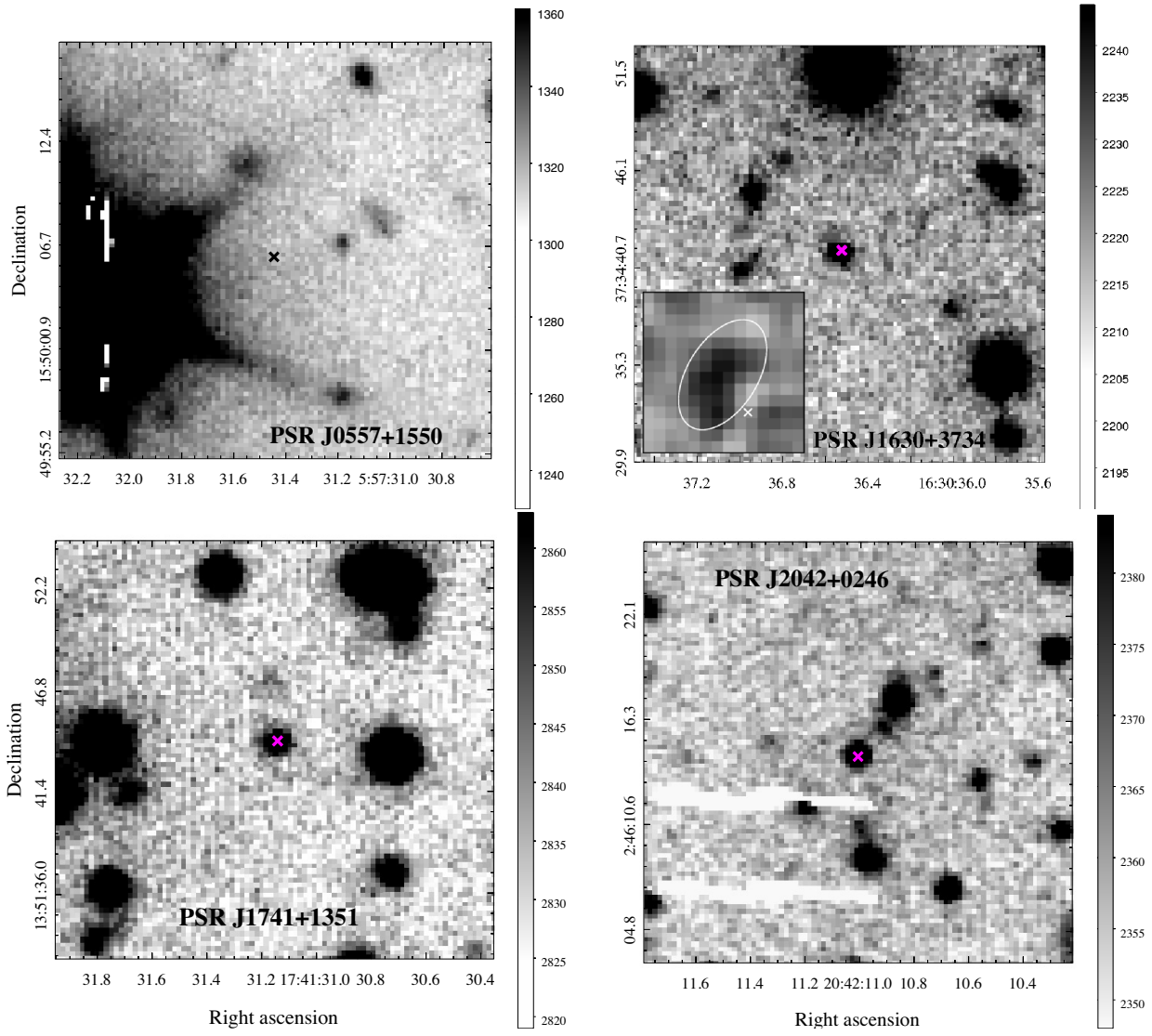

Figure 1. GTC/OSIRIS Sloan r'-band image fragments of the PSRs J0557+1550, J1630+3734, J1741+1351, and J2042+0246 fields. The crosses show the pulsar's radio positions for the epoch of the optical observations. The PSR J1630+3734 (3.5 × 3.5 arcsec^2) vicinity with the subtracted counterpart is enlarged in the left-hand bottom corner of the respective image fragment. The nearby extended source is enclosed in the ellipse and the position of the pulsar is marked by 'X' (see text for details). This fragment is smoothed with a 2-pixel Gaussian kernel. The two white stripes on the PSR J2042+0246 image are the detector defects. The astrometric uncertainties of the pulsar positions are negligible in the spatial scale of the images. The colour bar identifies the image values in 100 counts units.

4.2 PSR J1630+3734

In the colour–colour diagram, the PSR J1630+3734 companion shows a $\approx 2\sigma$ error displacement to bluer colour indices from the tracks of WDs with pure hydrogen or helium atmospheres (DA*, DA, and DB tracks; see the bottom panel of Fig. 2). The shift is not related to uncertainties of the DM distance as the extinction in the PSR J1630+3734 direction is very low (see Table 3) and does not affect the source intrinsic colours.

It is known that models of ultracool WDs with mixed He/H atmospheres show bluer $(g' - r')_0$ colours as opposed to those of WDs with pure hydrogen or helium atmospheres (e.g. Parsons et al. 2012). As an example, in Fig. 2 we also present the cooling tracks for CO-core WDs with mixed atmospheres (for log(He/H) $= 1.0$ and 4.0). The position of the PSR J1630+3734 companion is in accord with these tracks. Unfortunately, respective tracks for helium-core WDs are not available and at the current stage the determination of the presumed He/H ratio in the WD atmosphere is not possible. If the source is indeed a WD with a mixed atmosphere, its temperature and age are $\sim 4 \times 10^3$ K and ~2–5 Gyr, respectively. We note, however, that the $\sim 2\sigma$ displacement to bluer colour indices does not exclude the pure hydrogen or helium atmospheres, but makes them less plausible.

4.3 PSR J1741+1351

The temperature of the PSR J1741+1351 companion, assuming its WD nature and taking into account the intrinsic colour indices (see Fig. 2), is about $(6–7) \times 10^3$ K. This estimation is independent of any considered distance from Table 1 as $E(B - V)$ along the pulsar line of sight and the intrinsic colours of the companion vary only slightly within the expected distance range ≈0.9–2.3 kpc. The radio timing analysis by Arzoumanian et al. (2018) provides the parallax distance

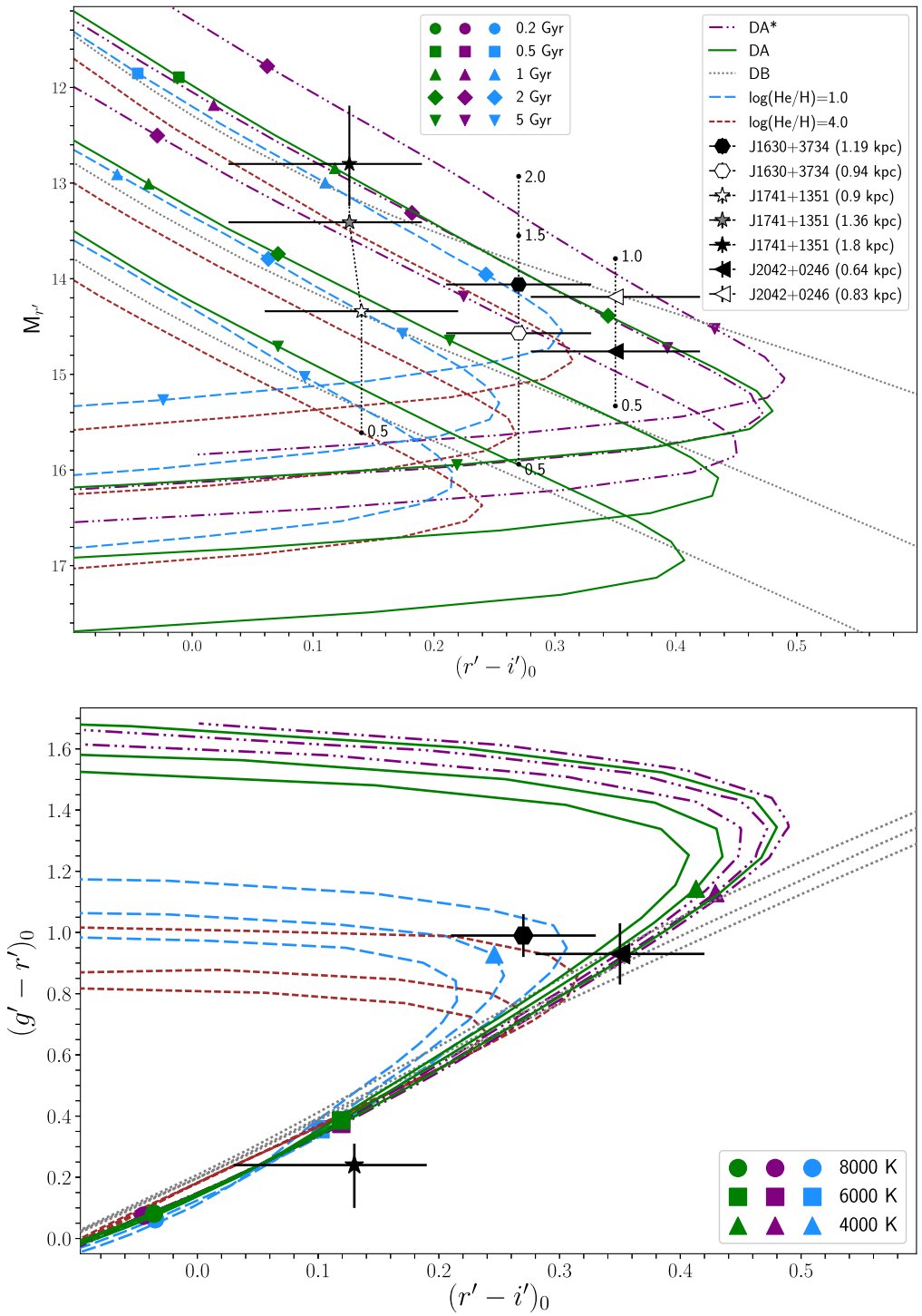

Figure 2. Colour–magnitude (top) and colour–colour (bottom) diagrams with various WD cooling tracks and data for WD companions to different MSPs listed in the legend. Purple dash-dot-dotted lines (DA*) show evolutionary tracks by Althaus et al. (2013) for helium-core WDs with masses 0.1821, 0.2724, and 0.4352 $M_\odot$. Solid green (DA) and grey dotted (DB) lines show models for CO-core WDs with hydrogen and helium atmospheres, respectively (Holberg & Bergeron 2006; Kowalski & Saumon 2006; Bergeron et al. 2011; Tremblay et al. 2011) with masses 0.2, 0.6, and 1.0 $M_\odot$. Dashed blue and brown lines are tracks for WDs with mixed atmospheres (log(He/H) $= 1.0$ and 4.0, respectively) and masses 0.2, 0.6, and 1.0 $M_\odot$. Masses increase from upper to lower tracks. WDs' ages (top) and effective temperatures (bottom) are shown by different symbols. The positions of the PSRs J1630+3734, J1741+1351, and J2042+0246 companions are shown by different symbols as indicated in the legend. In the top panel, for each source its positions are shown for different DM distance estimates (provided by the YMW16 and NE2001 models); for the PSR J1741+1351 companion the position corresponding to the timing parallax distance is also indicated (see Table 1). We also indicate their positions at various additional distances derived using reddening values from the dust map by Green et al. (2019). The distances are marked by the numbers in kpc units. Since their colours do not change significantly with the distance, in the lower panel the results are presented for the distances from Table 1.

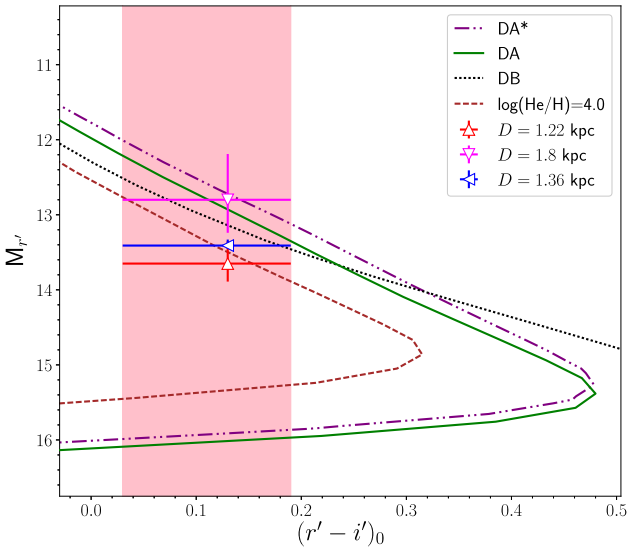

Figure 3. Colour–magnitude diagrams with WD cooling sequences. The dash-dot-dotted purple line (DA*) shows the track for a helium-core WD with a mass of 0.239 $M_\odot$ (Althaus et al. 2013), solid green (DA) and black dotted (DB) lines for CO-core WDs with masses of 0.2 $M_\odot$ with hydrogen and helium atmospheres, respectively (Holberg & Bergeron 2006; Kowalski & Saumon 2006; Bergeron et al. 2011; Tremblay et al. 2011), and the dashed brown line for a WD with mixed atmosphere (log(He/H) = 4.0) and a mass of 0.2 $M_\odot$. The positions of the PSR J1741+1351 optical companion are shown by triangle symbols for different distance estimates indicated in the legend. The pink stripe corresponds to the source $(r' - i')_0$ colour in the case of the maximum extinction in the pulsar direction.

to the pulsar $1.8^{+0.5}_{-0.3}$ kpc and the companion mass $M_c = 0.22(5)\ M_\odot$. The corresponding derived absolute magnitude and colour index of the companion are $M_{r'} = 12.80^{+0.44}_{-0.61}$ and $(r' - i')_0 = 0.13^{+0.06}_{-0.10}$. They are consistent with a hydrogen or helium atmosphere WD with a mass of 0.2–0.3 $M_\odot$ that is in agreement with the mass measurement from the radio timing. The respective WD cooling age is 1–2 Gyr (see Fig. 2). The DM distance $D_{\rm YMW16} = 1.36$ kpc based on the YMW16 model implies a helium or mixed He/H atmosphere WD with similar mass and age ranges, 0.2–0.5 $M_\odot$ and 1–2 Gyr, respectively. In contrast, the smaller DM distance $D_{\rm NE2001} = 0.9$ kpc requires an older (∼2–5 Gyr) and a more massive ($\gtrsim$0.4 $M_\odot$) WD.

Recently, Freire et al. (in preparation) have reported measurements of the PSR J1741+1351 system parameters based on new radio observations with high cadence in combination with publicly available data provided by NANOGrav (Demorest et al. 2013). They confirmed and improved the value for the companion mass $M_c = 0.227^{+0.014}_{-0.013}\ M_\odot$, provided the estimations on the pulsar mass $M_p = 1.19^{+0.11}_{-0.10}\ M_\odot$ and the parallactic distance $1.22^{+0.13}_{-0.11}$ kpc, however these are still preliminary. The new parallactic distance is marginally consistent with the DM distance $D_{\rm YMW16} = 1.36$ kpc and implies that the PSR J1741+1351 companion may have a mixed atmosphere. In Fig. 3, we present a colour–magnitude diagram with selected evolution tracks for WDs with different atmosphere compositions (DA, DB, and He/H) and masses that are close to the companion mass. At the distance $D = 1.22$ kpc, the companion perfectly agrees with a WD with a mixed He/H atmosphere.

Nevertheless, taking into account the formal distance and photometric measurements' uncertainty, a WD with a pure hydrogen or helium atmosphere is rather less plausible than completely rejected. As we mentioned before, $E(B - V)$ in the pulsar direction does not vary for the distances $\gtrsim$0.9 kpc (Green et al. 2019) and the companion colours do not change with the distance either. The stripe in Fig. 3 corresponds to the source intrinsic colour in case of the maximum $E(B - V)$. Pure hydrogen atmospheres of WDs provide higher luminosities and larger corresponding distances in a range of 1.5–2.7 kpc, whereas the mixed atmospheres require a distance between 1.1 and 1.52 kpc. Therefore, determining the distance to the system is critical to select the appropriate model of the companion atmosphere.

The DA and DB tracks in Figs 2 and 3 represent the CO-core WDs cooling models, while it is generally believed that low-mass WDs in MSP binaries have helium cores (Tauris 2011). Comparison of tracks for (DA*) helium-core and CO-core WDs with hydrogen atmospheres shows that at a given age and mass the latter ones are less luminous (van Oirschot et al. 2014). At ages $\gtrsim$1 Gyr for low-mass WDs the brightness difference becomes less than a half of a magnitude. As seen from Fig. 3, for the specific masses the difference between the DA and DA* tracks is even smaller and is comparable to the derived uncertainty in the absolute magnitude of the companion.

4.4 PSR J2042+0246

As it was mentioned before, most of the WD companions to MSPs have a pure hydrogen atmosphere. Positions of the PSR J2042+0246 companion on the colour–magnitude and colour–colour diagrams in Fig. 2 roughly correspond to a cool (≈4500 K) hydrogen-atmosphere WD with an age of ∼2–5 Gyr, depending on the cooling model.

To better constrain the WD parameters for this system, we utilized the procedure described by Dai et al. (2017) and used the models for helium-core hydrogen-atmosphere WDs with masses of 0.1554–0.4352 $M_\odot$ and the CO-core hydrogen-atmosphere WDs with masses of 0.5–1.0 $M_\odot$. The models were interpolated in the mass–temperature plane within a mass range of 0.1554–1.0 $M_\odot$ and a temperature range of 3000–10000 K using a 7000 × 7000 grid. Then the likelihood of each model point was calculated according to formula (5) from Dai et al. (2017). We assumed the distance range between $D_{\rm YMW16}$ and $D_{\rm NE2001}$, i.e. 0.6–0.8 kpc. As a result, we derived a WD mass of $0.30^{+0.07}_{-0.06}\ M_\odot$, a temperature of $4.49(14) \times 10^3$ K, and an age of $5.6^{+0.9}_{-1.2}$ Gyr (the values correspond to the medians of the probability distributions and their 1σ uncertainties). The obtained constraints on the WD mass and temperature are presented in Fig. 4.

The results show that the companion can indeed be a helium-core WD, as the derived mass lies within the mass range of the model set by Althaus et al. (2013). This mass is compatible with the lower limit $M_c > 0.19\ M_\odot$ provided by the radio timing measurements (Table 1). The derived WD mass and the mass function 0.0026721258 $M_\odot$ obtained by Sanpa-Arsa (2016) yield a lower limit on the pulsar mass of $\gtrsim$1.6 $M_\odot$ assuming a 'median' orbit inclination of 60°. In a specific case of 90°, the lower limit is $\gtrsim$2 $M_\odot$. This is in agreement with the fact that in MSP WD binaries neutron stars are on average more massive than in double pulsar systems, where the mass distribution of neutron stars shows a narrow peak around 1.35 $M_\odot$ (e.g. Linares 2019).

5 SUMMARY AND CONCLUSIONS

Using the GTC, we have performed optical observations of four binary MSPs. We have detected likely companions to

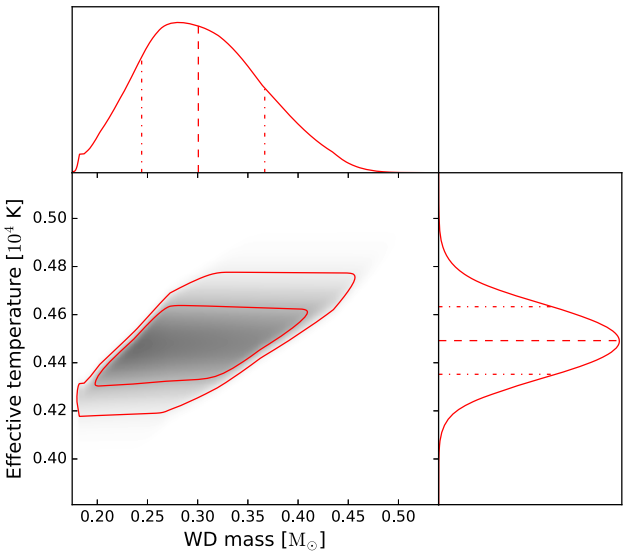

Figure 4. Constraints on the effective temperature and mass for the PSR J2042+0246 WD companion. The contours show the 68.3 and 95.5 per cent confidence levels. 1D likelihoods are shown in the top and side panels. Dashed lines indicate the median values and dash–dotted lines are the 1σ confidence intervals.

PSRs J1630+3734, J1741+1351, and J2042+0246 and set the upper limit on the PSR J0557+1550 companion brightness in the r' band, which is by ∼3.6 mag deeper than the previous one (Scholz et al. 2015). The magnitudes and colours of the detected optical sources are consistent with the evolutionary sequences of low-mass WDs, confirming the results from the radio timing measurements. Using the WD cooling sequences, we have constrained the parameters of the detected WD companions, including mass, temperature, and age. The latter two are presented in Table 3.

Colours of the PSR J1630+3734 companion suggest a WD with a mixed He/H atmosphere. The companion has a temperature of about 4×10^3 K and age of ∼2–5 Gyr.

The PSR J2042+0246 companion is consistent with an old ($\gtrsim$5 Gyr) helium-core hydrogen-atmosphere WD with a mass of $0.30^{+0.07}_{-0.06}$ $M_\odot$ and a temperature of $4.49(14) \times 10^3$ K. Assuming a median orbit inclination of 60°, we estimate the minimum pulsar mass to be 1.6 $M_\odot$.

For the PSR J1741+1351 system, the optical data and the WD cooling predictions suggest that the temperature of the companion is about $(6–7)\times 10^3$ K regardless of the distance, and its age is ∼1–2 Gyr. The latest parallactic and the $D_{\rm YMW16}$ distance estimations imply that the WD in the PSR J1741+1351 binary may have a mixed H/He atmosphere.

Mixed atmospheres in WDs are generally unusual since, due to gravitational settling, pure hydrogen atmospheres are expected (e.g. Althaus & Benvenuto 2000). Indeed, most of the known WD companions to MSPs are known to have hydrogen atmospheres. There are, however, several exceptions: the likely ultracool companions to PSRs J0751+1807 (Bassa, van Kerkwijk & Kulkarni 2006), J0740+6620 (Beronya et al. 2019), and J2017+0603 (Bassa et al. 2016), which may have pure helium or mixed atmospheres; the massive CO-core WD companion to the mildly recycled PSR B0655+64 (van Kerkwijk & Kulkarni 1995), which shows carbon lines in its spectrum. Based on the current data, it is possible that the companions to PSRs J1630+3734 and J1741+1351 can complement this set. In MSP binaries, WD hydrogen envelopes can be reduced due to irradiation by the pulsar wind following the cessation of the mass transfer (Ergma, Sarna & Gerškevitš-Antipova 2001). Indeed, the above-mentioned systems are close binaries ($P_{\rm b} \lesssim 5$ d) with a high pulsar spin-down power ($\dot{E} \sim 10^{34}$ erg s^{-1}), and it is clear that they can follow this scenario. However, since PSRs J1630+3734 and J1741+1351 possess longer orbital periods, this explanation is unlikely. To verify this we have obtained basic estimations on the companion flux and the flux of the pulsar wind irradiating the companion (see e.g. Bassa et al. 2016) for both systems. Indeed, the estimations yield a 1–2 orders of magnitude smaller irradiation fluxes in comparison with the companion ones implying that in case of PSRs J1630+3734 and J1741+1351 the irradiation could not have significantly altered the atmospheres of the companions.

Another possibility is that the WD companions to PSRs J1630+3734 and J1741+1351 have changed their atmospheric compositions from the hydrogen rich to the helium rich and back as they cooled down through the convective mixing stage (e.g. Chen & Hansen 2012): when the temperature decreases, the surface convection zone of hydrogen expands and can reach the underlying helium layer; then the convection brings helium to the surface. Moreover, other mechanisms changing a WD surface composition were proposed (see e.g. Blouin et al. 2019, and references therein).

Finally, we find that the WD ages in the PSRs J0557+1550, J1741+1351, and J2042+0246 binaries are consistent with the characteristic ages of their pulsar companions (see Table 1). In contrast, the PSR J1630+3734 intrinsic characteristic age $\tau_{\rm i}$, corrected for the Shklovskii and Galactic potential effects, is 6.1 ± 0.6 Gyr (Sanpa-Arsa 2016), which is somewhat larger than the estimated cooling age of the WD companion. However, characteristic ages are rough estimations and can significantly deviate from the true pulsar ages (see e.g. Lorimer & Kramer 2012). In addition, Tauris (2012) has shown that during the decoupling phase of the companion from its Roche lobe, rotational energy of the pulsar is dissipated. As a result, characteristic ages do not represent the true age of these neutron stars. For this reason, in case of PSR J1630+3734, we do not consider the WD and pulsar age inconsistency as a strong argument against the optical identification of the pulsar companion and present the WD cooling ages as independent estimations on the age of the binaries.

As the companions to PSRs J0557+1550, J1630+3734, and J2042+0246 are very cool, their future studies would mostly rely on broad-band near-infrared observations where hydrogen and helium WD atmospheres can be best resolved based on the spectral energy distribution (Blouin et al. 2019). For the warmer PSR J1741+1351 companion, optical/near-infrared spectroscopy with large-aperture ground-based telescopes or with the *James Webb Space Telescope* might be feasible to get new information on this interesting system, whose pulsar appears to have an unusually low mass.

ACKNOWLEDGEMENTS

We thank the anonymous referee for the useful comments that allowed us to improve this paper. We also thank P. Bergeron for providing cooling tracks for WDs with mixed atmospheres. The work is based on observations made with the Gran Telescopio Canarias (GTC), installed at the Spanish Observatorio del Roque de los Muchachos of the Instituto de Astrofísica de Canarias, in

the island of La Palma. IRAF is distributed by the National Optical Astronomy Observatory, which is operated by the Association of Universities for Research in Astronomy (AURA) under a cooperative agreement with the National Science Foundation. This work has made use of data from the European Space Agency (ESA) mission *Gaia* (https://www.cosmos.esa.int/gaia), processed by the *Gaia* Data Processing and Analysis Consortium (DPAC; https://www.cosmos.esa.int/web/gaia/dpac/consortium). Funding for the DPAC has been provided by national institutions, in particular the institutions participating in the *Gaia* Multilateral Agreement. This work also used public data from the North American Nanohertz Observatory for Gravitational Waves (NANOGrav; http://nanograv.org), which is designated as a 'Physics Frontiers Center' by the National Science Foundation (award # 1430284). DAZ thanks Pirinem School of Theoretical Physics for hospitality. The work of AYuK, AVK, and DAZ was supported by the Russian Foundation for Basic Research, project no. 18-32-20170 mol_a_ved. The work of SVZ was supported by PAPIIT grants IN-100617 and IN-102120.

REFERENCES

Alpar M. A., Cheng A. F., Ruderman M. A., Shaham J., 1982, Nature, 300, 728
Althaus L. G., Benvenuto O. G., 2000, MNRAS, 317, 952
Althaus L. G., Miller Bertolami M. M., Córsico A. H., 2013, A&A, 557, A19
Antoniadis J., 2014, ApJ, 797, L24
Antoniadis J., van Kerkwijk M. H., Koester D., Freire P. C. C., Wex N., Tauris T. M., Kramer M., Bassa C. G., 2012, MNRAS, 423, 3316
Antoniadis J. et al., 2013, Science, 340, 448
Arzoumanian Z. et al., 2018, ApJS, 235, 37
Bassa C. G., van Kerkwijk M. H., Kulkarni S. R., 2006, A&A, 450, 295
Bassa C. G., Antoniadis J., Camilo F., Cognard I., Koester D., Kramer M., Ransom S. R., Stappers B. W., 2016, MNRAS, 455, 3806
Bergeron P. et al., 2011, ApJ, 737, 28
Beronya D. M., Karpova A. V., Kirichenko A. Y., Zharikov S. V., Zyuzin D. A., Shibanov Y. A., Cabrera-Lavers A., 2019, MNRAS, 485, 3715
Bisnovatyi-Kogan G. S., Komberg B. V., 1974, SvA, 18, 217
Blouin S., Dufour P., Thibeault C., Allard N. F., 2019, ApJ, 878, 63
Chen E. Y., Hansen B. M. S., 2012, ApJ, 753, L16
Cordes J. M., Lazio T. J. W., 2002, preprint (arXiv:astro-ph/0207156)
Dai S., Smith M. C., Wang S., Okamoto S., Xu R. X., Yue Y. L., Liu J. F., 2017, ApJ, 842, 105
Demorest P. B. et al., 2013, ApJ, 762, 94
Ergma E., Sarna M. J., Gerškevitš-Antipova J., 2001, MNRAS, 321, 71
Espinoza C. M. et al., 2013, MNRAS, 430, 571
Freire P. C. C., Tauris T. M., 2014, MNRAS, 438, L86
Freire P., Jacoby B., Bailes M., Stairs I., Mott A., Ferdman R., Nice D., Backer D. C., 2006, Am. Astron. Soc. Meeting Abstr., #208, 72.06
Gaia Collaboration et al., 2016, A&A, 595, A1
Gaia Collaboration et al., 2018, A&A, 616, A1
Green G. M., Schlafly E. F., Zucker C., Speagle J. S., Finkbeiner D. P., 2019, ApJ, 887, 93
Holberg J. B., Bergeron P., 2006, AJ, 132, 1221
Jacoby B. A., Bailes M., Ord S. M., Knight H. S., Hotan A. W., 2007, ApJ, 656, 408
Kirichenko A. Y., Zharikov S. V., Zyuzin D. A., Shibanov Y. A., Karpova A. V., Dai S., Cabrera Lavers A., 2018, MNRAS, 480, 1950
Kowalski P. M., Saumon D., 2006, ApJ, 651, L137
Linares M., 2019, preprint (arXiv:1910.09572)
Lorimer D. R., Kramer M., 2012, Handbook of Pulsar Astronomy. Cambridge Univ. Press, Cambridge
Parsons S. G. et al., 2012, MNRAS, 426, 1950
Portegies Zwart S., van den Heuvel E. P. J., van Leeuwen J., Nelemans G., 2011, ApJ, 734, 55
Ray P. S. et al., 2012, preprint (arXiv:1205.3089)
Salvetti D. et al., 2017, MNRAS, 470, 466
Sanpa-Arsa S., 2016, PhD thesis, University of Virginia, (Available at: https://libraetd.lib.virginia.edu/public view/0k225b07h)
Schlafly E. F., Finkbeiner D. P., 2011, ApJ, 737, 103
Scholz P. et al., 2015, ApJ, 800, 123
Shapiro I. I., 1964, Phys. Rev. Lett., 13, 789
Smith J. A. et al., 2002, AJ, 123, 2121
Tauris T. M., 2011, in Schmidtobreick L., Schreiber M. R., Tappert C., eds, ASP Conf. Ser. Vol. 447, Evolution of Compact Binaries. Astron. Soc. Pac., San Francisco, p. 285
Tauris T. M., 2012, Science, 335, 561
Tremblay P.-E., Bergeron P., Gianninas A., 2011, ApJ, 730, 128
van Dokkum P. G., 2001, PASP, 113, 1420
van Kerkwijk M. H., Kulkarni S. R., 1995, ApJ, 454, L141
van Kerkwijk M. H., Bassa C. G., Jacoby B. A., Jonker P. G., 2005, in Rasio F. A., Stairs I. H., eds, ASP Conf. Ser. Vol. 328, Binary Radio Pulsars. Astron. Soc. Pac., San Francisco, p. 357
van Oirschot P., Nelemans G., Toonen S., Pols O., Brown A. G. A., Helmi A., Portegies Zwart S., 2014, A&A, 569, A42
Yao J. M., Manchester R. N., Wang N., 2017, ApJ, 835, 29
Zyuzin D. A., Kirichenko A. Yu., Karpova A. V., Shibanov Y. A., Zharikov S. V., Fonseca E., Cabrera-Lavers A., 2019, J. Phys.: Conf. Ser., 1400, 022013

This paper has been typeset from a TEX/LATEX file prepared by the author.